HHS Public Access

Author manuscript

Gene Ther. Author manuscript; available in PMC 2014 October 01.

Published in final edited form as:

Gene Ther. 2014 April ; 21(4): 379–386. doi:10.1038/gt.2014.7.

Effect of Bortezomib on the Efficacy of AAV9.SERCA2a Treatment to Preserve Cardiac Function in a Rat Pressure-Overload Model of Heart Failure

Antoine H. Chaanine, M.D.[#1], **Mathieu Nonnenmacher, Ph.D.**[#1], **Erik Kohlbrenner, B.Sc.**[1], **Dongzhu Jin, M.D.**[1], **Jason C. Kovacic, M.D.**[1], **Fadi G. Akar, Ph.D.**[1], **Roger J. Hajjar, M.D.**[1], and **Thomas Weber, Ph.D.**[1]

[1]Cardiovascular Research Center, Icahn School of Medicine at Mount Sinai, New York, NY 10029

[#] These authors contributed equally to this work.

Abstract

Adeno-associated virus (AAV)-based vectors are promising vehicles for therapeutic gene delivery, including for the treatment of heart failure. It has been demonstrated for each of the AAV serotypes 1 through 8 that inhibition of the proteasome results in increased transduction efficiencies. For AAV9, however, the effect of proteasome inhibitors on *in vivo* transduction has until now not been evaluated. Here we demonstrate, in a well-established rodent heart failure model, that concurrent treatment with the proteasome inhibitor bortezomib does not enhance the efficacy of AAV9.SERCA2a to improve cardiac function as examined by echocardiography and pressure volume analysis. Western blot analysis of SERCA2a protein and RT-PCR of SERCA2a mRNA demonstrated that bortezomib had no effect on either endogenous rat SERCA2a levels nor on expression levels of human SERCA2a delivered by AAV9.SERCA2a. Similarly, the number of AAV9 genomes in heart samples was unaffected by bortezomib treatment. Interestingly, whereas transduction of HeLa cells and neonatal rat cardiomyocytes by AAV9 was stimulated, transduction of adult rat cardiomyocytes was inhibited. These results indicate an organ/cell-type specific effect of proteasome inhibition on AAV9 transduction. A future detailed analysis of the underlying molecular mechanisms promises to facilitate the development of improved AAV vectors.

Keywords

Adeno-associated virus; AAV; gene therapy; heart failure; bortezomib; proteasome inhibitors

Address correspondence to: Dr. Thomas Weber Cardiovascular Research Center, Icahn School of Medicine at Mount Sinai One Gustave L. Levy Place, Box 1030 New York, NY 10029 thomas.weber@mssm.edu Phone: 212-241-0282 Fax: 646-537-9458.

Conflict of Interest

Dr. Hajjar is the scientific cofounder of Celladon, which plans to commercialize AAV1.SERCA2a for the treatment of heart failure. All other authors declare no competing financial interest.

Introduction

Adeno-associated virus-based vectors are increasingly used as gene transfer vectors in both preclinical disease models as well as clinical trials[1]. This is in part due to the lack of pathogenicity of adeno-associated viruses (AAVs), their comparatively low immunogenicity and the ability of recombinant AAVs to cause long-term transgene expression even in the absence of genome integration, at least in non-dividing cells[1].

Excitingly, in Europe, AAV gene therapy has recently been approved for the treatment of lipoprotein lipase deficiency[2] thus bringing AAV gene therapy to the clinic. Other promising results in clinical trials have been obtained in the treatment of ocular diseases, such as inherited retinopathies (reviewed in[3]) and blood clotting disorders, namely factor IX deficiency[4]. Furthermore, we and others have shown that the overexpression of the sarco/endoplasmatic calcium ATPase, SERCA2a, can ameliorate heart failure in both small[5, 6] and large animal models[7-9]. Based on these preclinical data, a first-in-man phase I-II clinical trial for patients with advanced heart failure using AAV-based vectors encoding SERCA2a was initiated and recently concluded[10, 11]. This so-called CUPID trial showed that injection of high dose AAV1.SERCA2a decreased clinical events in patients with heart failure.

While these early results from clinical trials show promise, these trials also brought to light challenges that must be overcome in order to implement broadly AAV gene transfer as a therapeutic modality. Among the difficulties encountered is the need for large vector doses to achieve sufficient transduction efficiencies. The requirement for large vector doses is not only challenging in terms of GMP level AAV vector production but—maybe more importantly—in some trials, large vector doses have been shown to trigger a cellular immune response against the AAV capsids[12, 13].

It is not surprising then that intense research is taking place to improve transduction efficiencies by isolating new AAV genotypes[14, 15], by modifying the AAV capsid by both site-directed[16] and directed evolution approaches[16, 17] as well as by using drugs that enhance AAV transduction (see[18]). These drugs include tyrosine kinase inhibitors[19], topoisomerase inhibitors[19-21], genotoxic agents, such as hydroxyurea[20, 22, 23] and proteasome inhibitors[24-28]. Proteasome inhibitors are of particular interest as they not only increase transduction by all serotypes studied today[24-28] but recently have been demonstrated to lead to a reduced presentation of AAV capsid-derived peptides on MHC class I molecules[29] thus reducing the risk of an immune response against transduced cells. A number of studies showed that proteasome inhibitors can enhance transduction by AAV serotypes 1 through 8[24-28]. Most recently, it was also shown that proteasome inhibitors can increase AAV9 transduction *in vitro*[30], but the effect of proteasome inhibitors on transduction by AAV9 *in vivo* has so far not been reported. Hence, we decided to test if the FDA approved proteasome inhibitor bortezomib (also known as Velcade®) can increase the efficiency of AAV9.SERCA2a in improving cardiac function in a rat model of pressure overload induced heart failure.

Results

For our studies we used a rat pressure overload model[31], in which heart failure (HF) is induced by banding of the ascending aorta (study design: Figure 1A). Echocardiography was employed to assess left ventricular (LV) dimensions and function. Systolic heart failure was observed between eight and twelve weeks after aortic banding. Once HF developed, animals were randomized to receive via tail vein injection 1×10^{12} genome containing particles (gcp) of AAV9.SERCA2a alone, 1×10^{12} gcp AAV9.SERCA2a plus bortezomib or an equivalent amount of empty AAV9 particles. As reported previously[32], the maximal tolerated dose of bortezomib in rats was 0.1 mg/kg. At doses of 0.3 mg/kg or 0.5 mg/kg some animals died within one week of injection. A dose of 0.1 mg/kg of bortezomib, however, was well tolerated in both sham-treated animals and animals with HF. Two months after vector injection cardiac function was assessed noninvasively by echocardiography and invasively using pressure-volume loop measurements (Figure 1A). At the time of sacrifice, heart and body weight were also measured.

The heart weight to body weight ratio was significantly increased in the HF animals (AAV9.Empty, AAV9.SERCA2a and the AAV9.SERCA2a plus bortezomib groups) compared to sham operated animals (Table 1). Left ventricular (LV) septal wall thickness as well as LV posterior wall thickness gradually increased in the first few weeks after ascending aortic banding (AAB) and reached maximum at about 4 weeks after AAB (data not shown) and was preserved up until the onset of HF. At two months, the thickness of the septal and posterior wall remained about the same in all vector-injected animals compared to the time of onset of HF and was significantly higher than the sham operated animals. (Figure 1-B and Table 1).

The echocardiography data shown in Figure 1C and in Table 1 also demonstrate that two months after treatment, LV end-systolic (LVESV) and LV end-diastolic (LVEDV) volumes were significantly lower in the AAV9.SERCA2a, with or without bortezomib treated groups compared to AAV9.Empty treated group (Figure 1C). Also, LV fractional shortening and LV ejection fraction were significantly higher in the above two groups compared to the AAV9.empty treated animals (Table 1). Unexpectedly, however, there were no differences in LV diameters and LV volumes or in LV fractional shortening and LV ejection fraction between the AAV9.SERCA2a and the AAV9.SERCA2a plus bortezomib treated groups. Hemodynamic measurements, by P-V loop, were conducted at baseline and during LV unloading by inferior vena cava (IVC) occlusion (Table 2). Figure 2-A and Figure 2-B are showing P-V loop tracings at baseline and during IVC occlusion, respectively. Compared to the AAV9.Empty treated group there were significant decreases in LVEDV and LVSEV as well as a significant increase in LV ejection fraction in the AAV9.SERCA2a and AAV9.SERCA2a plus bortezomib treated animals (Figure 2-C and Table 2). However, consistent with the echocardiographic data, there were no significant differences in the hemodynamic parameters between the AAV9.SERCA2a and the AAV9.SERCA2a plus bortezomib treated groups. LV contractility, as measured by the End Systolic Pressure Volume Relationship (ESPVR) during LV unloading by IVC occlusion, was significantly higher in the AAV9.SERCA2a and AAV9.SERCA2a plus bortezomib groups, with a significant shift of V0 to the left, compared to AAV9.Empty injected rats. The significant

leftward shift of V0 seen in the AAV9.SERCA2a and in the AAV9.SERCA2a plus bortezomib group is attributed to the reversal of cardiac remodeling with significantly lower LV end diastolic and LV end systolic volumes (Figure 2-D and Table 2).

LV End Diastolic Pressure Volume Relationship (EDPVR), obtained during LV unloading by IVC occlusion, revealed no significant differences among the AAV9.Empty and AAV9.SERCA2a groups, with or without bortezomib, indicating that despite the significant improvement in LV contractility, there were no apparent benefits in LV stiffness or LV relaxation among these groups. There was, however, a trend towards improved LVEDP and EDPVR and a trend toward decreased interstitial fibrosis (data not shown) in the AAV9.SERCA2a group compared to HF + AAV9.Empty group.

The lack of increased efficacy in the AAV9.SERCA2a bortezomib group compared to the AAV9.SERCA2a alone group led us to compare the expression levels of SERCA2a in the treatment and control groups. As expected, SERCA2a expression was significantly decreased in the HF animals injected with empty AAV9 particles compared to the sham operated control group (Figure 3). Similarly, treatment of HF animals with AAV9.SERCA2a, with or without bortezomib, resulted in a significant restoration of SERCA2a expression (Figure 3). Surprisingly, however, there was no difference in SERCA2a protein levels between the AAV9.SERCA2a and the AAV9.SERCA2a plus bortezomib groups suggesting that either bortezomib depresses endogenous SERCA2a levels, or that AAV9 transduction is not enhanced in the presence of proteasome inhibitors, at least in rat hearts. To distinguish between these two possibilities we first determined the levels of endogenous, rat SERCA2a mRNA by RT-PCR. Interestingly, consistent with previous observations[8] and in contrast to SERCA2a protein levels, there was no difference among any of the groups, including among sham treated animals and animals with heart failure injected with AAV9 capsids (Figure 4A). These results suggest that bortezomib does not influence endogenous SERCA2a mRNA levels, and that the observed decrease in SERCA2a protein levels is a result of enhanced SERCA2a degradation[5]. We next examined if the levels of human SERCA2a mRNA, encoded by AAV9.SERCA2a, were increased in bortezomib treated animals compared to animals injected with AAV9.SERCA2a alone. Surprisingly, there was a trend towards reduced human SERCA2a expression in the bortezomib treated animals, although this did not reach statistical significance (Figure 4B). Because the increase in transduction by proteasome inhibitors observed with other serotypes is thought to be, at least in part, a result of the stabilization of AAV virions, resulting in increased vector genomes in the transduced tissue, we next analyzed the presence of AAV9.SERCA2a genomes. In agreement with our transcription results, we did not see an increase in AAV9.SERCA2a genomes in rats treated with bortezomib compared to rats that had been injected with AAV9.SERCA2a alone. In contrast, there was a trend towards fewer AAV9.SERCA2a genomes in bortezomib treated animals, although this did not reach statistical significance (Figure 4C). Together, our results demonstrate that in rat hearts AAV9 transduction is not increased with the proteasome inhibitor bortezomib.

There are two obvious reasons for these results: 1) In contrast to other AAV serotypes, inhibition of proteasome activity does not increase AAV9 transduction, or 2) the lack of an increase in transduction by AAV9 is specific to rat cardiomyocytes. To distinguish between

these two possibilities we first analyzed the effect of bortezomib on AAV9 transduction in HeLa cells. Consistent with recently reported results[30], bortezomib treatment resulted in an approximately 10-fold and 20-fold increase in transduction by AAV9 and AAV2 respectively (Fig. 5A). These results demonstrate that similarly to other serotypes, proteasome inhibition can increase AAV9 transduction, at least in HeLa cells, thus ruling out that the lack of increased transduction is AAV9-specific. Rather, these results suggest that the lack of an increase in transduction is specific to rat cardiomyocytes. To test this hypothesis we analyzed the effect of bortezomib on AAV2, AAV6 and AAV9 transduction in neonatal rat cardiomyocytes and adult rat cardiomyocytes. Interestingly, bortezomib enhanced transduction of neonatal rat cardiomyocytes by AAV2, AAV6 and AAV9 by ~10-, ~2- and ~15-fold respectively (Fig. 5B). Strikingly—and in line with the *in vivo* data—bortezomib did not enhance AAV9 transduction in adult rat cardiomyocytes (Fig. 5C). In contrast, bortezomib treatment resulted in an approximately 10-fold reduction in AAV9 transduction and decreased transduction by AAV2 and AAV6 by ~25- and ~15-fold respectively. The reason for this decrease in transduction is unknown, but these results demonstrate that the effect of bortezomib on AAV transduction is not species-specific but rather cell type-specific.

Discussion

Both in small[6] and large animal models[8, 33] treatment of heart failure by overexpressing SERCA2a with AAV-based vectors has been shown to be successful at improving cardiac dysfunction. Furthermore, a recently completed phase I-II clinical trial for the treatment of advanced heart failure with AAV1.SERCA2a yielded encouraging results[10, 11]. Despite—or perhaps because of—these promising results, further improvements in cardiac delivery with AAV-based vectors remains an essential focus of investigation. For both safety and efficacy reasons, high-level expression of SERCA2a with the smallest possible vector dose remains an important goal.

In 2001, Danos and colleagues demonstrated that AAV2 transduction can be greatly enhanced by treating cells with the proteasome inhibitor MG132[24-28]. To date, there is no clear understanding of the exact mechanism by which proteasome inhibitors enhance AAV transduction. It was initially proposed that proteasome inhibitors increased AAV-mediated transduction simply by protecting viral capsids against cytoplasmic degradation, but subsequent investigations suggested that additional mechanisms were involved, including enhanced AAV trafficking to the nucleus[34] and mobilization in and out of the nucleolus[35].

Since the original observation by Danos et al.[26] with AAV2, an enhancement of transduction by proteasome inhibitors has been demonstrated for all of the serotypes 1 through 8[24-28]. Most recently, it has also been reported that bortezomib can increase AAV9 transduction *in vitro*[30]. But, to our knowledge, the effect of proteasome inhibitors on AAV9 transduction *in vivo* has so far not been evaluated[30]. Here we demonstrate that transduction of rat hearts by AAV9 is not enhanced at the maximum tolerated dose of bortezomib. The easiest explanation for this lack of enhancement of transduction would be that the bortezomib dose was too low. We deem this unlikely, however, because a slightly higher (and presumably toxic) dose of 0.2 mg/kg results in a rapid, profound (>80%) and prolonged

(≥72 hrs) inhibition of rat proteasome activity *in vivo* (Fig. 1 in[32]). Furthermore, bortezomib significantly inhibits transduction of adult rat cardiomyocytes (Fig. 5C), demonstrating that bortezomib can enter adult rat cardiomyocytes and presumably inhibit proteasome activity.

An alternative reason for the lack of enhanced transduction with bortezomib is that the effect of proteasome inhibitors on transduction is serotype-specific, possibly because the AAV9 capsid might be inherently more resistant to proteasomal degradation. Serotype-specific effects of proteasome inhibitors on AAV transduction have been reported in vascular endothelial cells where AAV2 transduction is greatly enhanced by LnLL and MG132, but transduction by AAV7 or AAV8 are unaffected[25]. However, our data do not support the conclusion that proteasome inhibitors act in a serotype-specific manner as bortezomib treatment had a similar effect on transduction by AAV2 and AAV9 in each cell type. Rather, our results indicate that bortezomib modulates AAV transduction in a cell-specific manner, since the same drug treatment had diametrically opposed effects on AAV transduction of neonatal versus adult rat cardiomyocytes reminiscent of the previously reported[25] cell-specific effect of MG132 on transduction by AAV8 and AAV7. Interestingly, surface tyrosine to phenylalanine mutants of AAV9, which would be expected to be more resistant to proteasomal degradation, show increased transduction of retinal tissue[36] but not cardiac or skeletal muscle[37], also indicating tissue-specific differences.

Taken together, our data demonstrate that transduction of (adult) rat cardiomyocytes cannot be increased by the proteasome inhibitor bortezomib either *in vivo* or *in vitro*. At present, it is unclear why bortezomib fails to enhance AAV9 transduction of rat myocardium and decreases AAV2, AAV6 and AAV9 transduction of isolated adult rat cardiomyocytes. Nor is it apparent why bortezomib stimulates transduction of neonatal rat cardiomyocytes by these AAV serotypes. It is clear, however, that serotype-specific or species-specific effects of bortezomib cannot explain the results. Rather the differences appear to be cell type-specific. A dissection of the biological basis for the lack of enhancement of AAV9 transduction of rat myocardium by bortezomib is beyond the scope of this manuscript. But the differential effects of bortezomib on AAV9 transduction of adult and neonatal rat cardiomyocytes provides us and others with an *in vitro* system to start dissecting the multifaceted mechanisms of proteasome inhibition on AAV transduction in various cell types and tissues. Thus, while it might be disappointing that proteasome inhibition does not result in increased heart transduction with AAV9 vectors, a dissection of the complex processes at work may reveal novel and important mechanistic insights that will facilitate the development of future AAV vectors with higher infectivities and/or better defined tissue tropism.

Material and Methods

Study Design and Induction of Heart Failure by Aortic Banding

All procedures involving the handling of animals were approved by the Animal Care and Use Committee of the Icahn School of Medicine at Mount Sinai and adhered with the Guide for the Care and Use of laboratory Animals published by the National Institutes of Health. The aortic banding model was used to generate pressure overload induced hypertrophy and heart failure. Sprague-Dawley rats weighing 180-200 g underwent ascending aortic banding

(AAB), as previously described in detail in[38]. For the heart failure experiment, animals that developed systolic heart failure were randomized to receive an injection of AAV9.Empty (n=5) vs. AAV9.SERCA2a (n=5) vs. AAV9.SERCA2a + bortezomib (Velcade®, Millenium, Cambridge MA) (n=3) for two months. Age matched sham operated animals were used as control (n=3). The viral dose used was 1×10^{12} genome containing particles (gcp) and the bortezomib dose used was 0.1 mg/kg. The virus and the bortezomib were injected simultaneously via the tail vein.

Echocardiography

Transthoracic echocardiography was performed using a Vivid 7 echocardiography apparatus with a 14 MHz probe (i13L probe, General Electric, New York, NY). Animals were sedated with ketamine 80-100 mg/kg injected intraperitoneally. Long and short axis parasternal views and short axis parasternal two dimensional (2D) views, at the mid-papillary level, of the left ventricle (LV) were obtained to calculate the LV end diastolic (LVEDV) and end systolic (LVESV) volumes as well as the ejection fraction of the LV (LVEF). Volumes were calculated by using the formulae of the area length method ($V=5/6\times A\times L$, where V: is the volume in ml, A: is the cross sectional area of the LV cavity in cm^2, obtained from the mid-papillary short parasternal image in diastole and in systole, and L: is the length of the LV cavity in cm, measured from the long parasternal axis image as the distance from the endocardial LV apex to the mitral-aortic junction in diastole and in systole). M-mode images were obtained by 2D guidance from the parasternal short axis view for the measurements of LV wall thickness of the interventricular septum (IVSd, cm) and the posterior wall (LVPWd, cm), LV end diastolic diameter (LVIDd, cm) and LV end systolic diameter (LVIDs, cm) as well as to calculate the LV fractional shortening (LVFS, %).

Invasive pressure-volume loop measurements of the left ventricle

At the study end point, LV pressure-volume loop measurements were obtained as previously described[39]. Briefly, rats were anesthetized with inhaled 5% (volume/volume) isoflurane for induction, and subsequently intubated and mechanically ventilated in an identical fashion to the aortic banding model and as described previously[38]. Isoflurane was lowered to 2 - 3% (volume/volume) for surgical incision. The chest was opened through a median sternotomy. A 1.9F rat P-V catheter (Scisense, London, Ontario, Canada) was inserted into the LV apex through an apical puncture performed with a 25G needle. Hemodynamic recordings were performed after 5 minutes of stable heart rate. Anesthesia was maintained at 0.75-1% isoflurane to keep the animal sedated and maintain a stable heart rate around 350 beats/minute. Hemodynamics were recorded subsequently through a Scisense P-V Control Unit (FY897B). The intrathoracic inferior vena cava was transiently occluded to decrease venous return during the recording to obtain load-independent P-V relationships. Linear fits were obtained for end-systolic pressure volume relationships (ESPVR) and end-diastolic pressure-volume relationships (EDPVR). At the end of the experiment, 50 μl of 30% NaCl was slowly injected into the external jugular vein for ventricular parallel conductance (Gp) measurement as previously described[39, 40]. Blood resistivity was measured using a special probe (Scisense). Volume measurements were initially obtained as blood conductance and calibrated using the Baan equation[41], and pressure sensors were calibrated as per manufacturer's instructions.

AAV Vector Production, Purification and Characterization

AAV9.SERCA2a contains a SERCA2a expression cassette flanked by two AAV2 inverted terminal repeats (ITRs) and is pseudotyped with an AAV9 capsid. The SERCA2a expression cassette consists of a CMV promoter followed by the human SERCA2a coding sequence and a SV40 polyadenylation signal. AAV9.SERCA2a was produced in 293 cells with the two plasmid method[42] and polyethyleneimine[43, 44]. The virus was purified by double iodixanol purification[44] followed by dialysis against lactated Ringer's solution. Vector purity, genome containing particle and viral particle titers were determined as described[44]. For *in vitro* experiments, a reporter cassette encoding firefly luciferase under the control of CAG promoter was packaged into AAV2, AAV6 or AAV9 capsids and purified on single iodixanol gradients[44] to yield AAV2-Luc, AAV6-Luc or AAV9-Luc virus.

Western Blotting

Protein lysates were obtained from left ventricular tissue that was homogenized in RIPA lysis and extraction buffer which contained protease and phosphatase inhibitors (Pierce, Rockford, IL, USA). Twenty micrograms of total protein extracts were mixed with Laemmli sample buffer containing 5% β-mercaptoethanol (Bio-Rad, Hercules, CA, USA). Samples were heated at 95 °C for 5 minutes and then loaded onto 12% SDS-PAGE gels. After electrophoresis proteins were transferred onto PVDF Membrane (Millipore, Billerica, MA, USA). Membranes were blocked with 5% fat-free milk in Tris-buffered saline (TBS) for 1 hour at room temperature and incubated with the primary antibodies diluted in blocking buffer overnight at 4°C. The following primary antibodies were used: GAPDH (Sigma, St. Louis, MO, USA 1:10000 dilution) and SERCA2a (21st Century Biochemicals, 1:3000 dilution, Marlboro, MA, USA). The second day, after three washing steps with TBS-0.05% Tween-20, the membrane was incubated with secondary fluorescent anti-mouse and anti-rabbit antibodies (LI-COR, Lincoln, NE, USA, 1:10,000 dilution) for 45 minutes then was washed three times with TBS- 0.05% Tween-20. The membrane was then scanned with an Odyssey imaging system (LI-COR Biosciences, Lincoln, NE, USA) and bands were analyzed with Odyssey software, version 3.0. The values obtained were normalized to GAPDH to correct for variation in protein loading.

Quantitation of Vector DNA and RNA in Tissue Samples

Frozen heart samples from rats injected with AAV9.SERCA2a or AAV9 empty capsids were ground in liquid nitrogen and stored at –80°C until extraction. Total DNA and RNA were purified from ~30 mg of tissue using Dneasy blood and tissue kit and Rneasy mini kit from Qiagen (Germantown, MD), respectively. RNA extraction included on-column digestion with RNAse-free DNAse (Qiagen; Germantown, MD) to prevent carryover of low-molecular weight viral DNA. RNA was reverse transcribed using Superscript® III kit (Life Technologies; Carlsbad, CA) using an oligo dT primer.

DNA and cDNA samples were then analyzed using SYBR® Advantage qPCR Master Mix (Clontech; Mountainview, CA) in an ABI 7500 Real-time PCR system.

Viral DNA was quantified using primers specific for human SERCA2a cDNA (hSERCA2a fwd: 5’-GGTTAACTTCCATCAAATCTACCACACTA-3’ and hSERCA2a rev: 5’-

CAATTTCGGTGTTAACTCCAGTTGCT-3'), spanning a 5-kb intron to prevent nonspecific amplification of rat genomic SERCA2a. Primers specific for an intron in the rat SERCA2a gene (forward 5'-TGTGCTCATGTGCTTGCTTCTTGG-3' and reverse 5'-AGCATTACCAAGTGCTCAGGACGA-3') were used to standardize the number of rat genomes present in each sample.

AAV-encoded human SERCA2a RNA was quantified after reverse transcription from cDNA samples with the same primer pair used for viral DNA. Endogenous rat SERCA2a mRNA was quantified after reverse transcription with primers specific for rat SERCA2a that showed no cross-reaction with the human SERCA2a (rSERCA2a fwd: 5'-ATTGACATCCATCAAGTCTACAACTCTG-3' and rSERCA2a rev: 5'-ATCTCAGTATTGACTCCAGTCGCC-3'). Rat GAPDH mRNA was quantified after reverse transcription with the primers rGAPDH fwd: 5'-ACAAGATGGTGAAGGTCGGTGTGA-3' and rGAPDH rev: 5'-AGCTTCCCATTCTCAGCCTTGACT-3' and was used to normalize the RNA content of all samples.

In vitro transduction assays

HeLa cells were obtained from American Type Culture Collection (Manassas, VA) and cultured in DMEM with 10% fetal bovine serum and penicillin/streptomycin, rat neonatal cardiomyocytes were isolated with the Neonatal Cardiomyocyte Isolation System from Worthington (Lakewood, NJ) according to the manufacturers instructions and plated on laminin-coated plates in medium (F10, 10% horse serum, 5% bovine serum, 100 i.u./ml penicillin, 100 μg/ml streptomycin). Rat adult cardiomyocytes were isolated by standard procedures[45] and plated on laminin-coated plates in DMEM, 132 μg/ml BSA, 20 μM glutamine, 100 i.u./ml penicillin, 100 μg/ml streptomycin, 1% insulin-transferrin-selenium-ethanolamine (Life-Technologies, Grand Island, NY; cat. no. 51500-056), 200 μM BDM (butanedione monoxime). Transduction assays were performed 16h post-isolation for neonatal cardiomyocytes and 3h post-isolation for adult cardiomyocytes. Cells were pre-treated for 30 minutes with 1 μM bortezomib (1.25 μM for HeLa cells) or with 0.01% DMSO and infected with AAV1-Luc, AAV2-Luc, AAV6-Luc or AAV9-Luc at an MOI of 1e4 vg/cell. Lysates were obtained after 24h for HeLa cells or 48h for both neonatal and adult cardiomyocytes, and luciferase activity was measured using luciferase assay reagent (Promega; Madison, WI) and a Synergy 2 plate reader (Biotek; Winooski, VT).

Statistical analysis

Results are shown as mean ± Standard Deviation. Statistical significance was determined using Student–Newman–Keuls test. A P value of < 0.05 was considered statistically significant.

Acknowledgments

This work was supported by NIH R01 HL093183 (RJH), HL088434 (RJH), HL097108 (FGA), P20 HL100396 (RJH), P50 HL112324 (RJH), NHLBI Program of Excellence in Nanotechnology (PEN) Award, contract number HHSN268201000045C (Zahi Fayad, Mount Sinai) and K08 HL111330 (JCK).

References

1. Mingozzi F, High KA. Therapeutic in vivo gene transfer for genetic disease using AAV: progress and challenges. Nat Rev Genet. 2011; 12(5):341–55. [PubMed: 21499295]
2. Gruber K. Europe gives gene therapy the green light. Lancet. 2012; 380(9855):e10. [PubMed: 23166921]
3. Colella P, Auricchio A. Gene Therapy of Inherited Retinopathies: A Long and Successful Road from Viral Vectors to Patients. Hum Gene Ther. 2012
4. Nathwani AC, Tuddenham EG, Rangarajan S, Rosales C, McIntosh J, Linch DC, et al. Adenovirus-associated virus vector-mediated gene transfer in hemophilia B. N Engl J Med. 2011; 365(25): 2357–65. [PubMed: 22149959]
5. Kho C, Lee A, Jeong D, Oh JG, Chaanine AH, Kizana E, et al. SUMO1-dependent modulation of SERCA2a in heart failure. Nature. 2011; 477(7366):601–5. [PubMed: 21900893]
6. Sakata S, Lebeche D, Sakata N, Sakata Y, Chemaly ER, Liang LF, et al. Restoration of mechanical and energetic function in failing aortic-banded rat hearts by gene transfer of calcium cycling proteins. J Mol Cell Cardiol. 2007; 42(4):852–61. [PubMed: 17300800]
7. Byrne MJ, Power JM, Preovolos A, Mariani JA, Hajjar RJ, Kaye DM. Recirculating cardiac delivery of AAV2/1SERCA2a improves myocardial function in an experimental model of heart failure in large animals. Gene Ther. 2008; 15(23):1550–7. [PubMed: 18650850]
8. Kawase Y, Ly HQ, Prunier F, Lebeche D, Shi Y, Jin H, et al. Reversal of cardiac dysfunction after long-term expression of SERCA2a by gene transfer in a pre-clinical model of heart failure. J Am Coll Cardiol. 2008; 51(11):1112–9. [PubMed: 18342232]
9. Mi YF, Li XY, Tang LJ, Lu XC, Fu ZQ, Ye WH. Improvement in cardiac function after sarcoplasmic reticulum Ca2+-ATPase gene transfer in a beagle heart failure model. Chin Med J (Engl). 2009; 122(12):1423–8. [PubMed: 19567165]
10. Jaski BE, Jessup ML, Mancini DM, Cappola TP, Pauly DF, Greenberg B, et al. Calcium upregulation by percutaneous administration of gene therapy in cardiac disease (CUPID Trial), a first-in-human phase 1/2 clinical trial. J Card Fail. 2009; 15(3):171–81. [PubMed: 19327618]
11. Jessup M, Greenberg B, Mancini D, Cappola T, Pauly DF, Jaski B, et al. Calcium Upregulation by Percutaneous Administration of Gene Therapy in Cardiac Disease (CUPID): A Phase 2 Trial of Intracoronary Gene Therapy of Sarcoplasmic Reticulum Ca2+-ATPase in Patients With Advanced Heart Failure. Circulation. 2011; 124(3):304–313. [PubMed: 21709064]
12. Mingozzi F, High KA. Immune responses to AAV in clinical trials. Curr Gene Ther. 2011; 11(4): 321–30. [PubMed: 21557723]
13. Mingozzi F, Maus MV, Hui DJ, Sabatino DE, Murphy SL, Rasko JE, et al. CD8(+) T-cell responses to adeno-associated virus capsid in humans. Nat Med. 2007; 13(4):419–22. [PubMed: 17369837]
14. Gao G, Vandenberghe LH, Wilson JM. New recombinant serotypes of AAV vectors. Current gene therapy. 2005; 5(3):285–97. [PubMed: 15975006]
15. Gao GP, Alvira MR, Wang L, Calcedo R, Johnston J, Wilson JM. Novel adeno-associated viruses from rhesus monkeys as vectors for human gene therapy. Proc Natl Acad Sci U S A. 2002; 99(18): 11854–9. [PubMed: 12192090]
16. Michelfelder S, Trepel M. Adeno-associated viral vectors and their redirection to cell-type specific receptors. Adv Genet. 2009; 67:29–60. [PubMed: 19914449]
17. Bartel MA, Weinstein JR, Schaffer DV. Directed evolution of novel adeno-associated viruses for therapeutic gene delivery. Gene Ther. 2012; 19(6):694–700. [PubMed: 22402323]
18. Nonnenmacher M, Weber T. Intracellular transport of recombinant adeno-associated virus vectors. Gene Ther. 2012; 19(6):649–58. [PubMed: 22357511]
19. Zhong L, Zhao W, Wu J, Li B, Zolotukhin S, Govindasamy L, et al. A Dual Role of EGFR Protein Tyrosine Kinase Signaling in Ubiquitination of AAV2 Capsids and Viral Second-strand DNA Synthesis. Mol Ther. 2007; 15(7):1323–1330. [PubMed: 17440440]
20. Russell DW, Alexander IE, Miller AD. DNA synthesis and topoisomerase inhibitors increase transduction by adeno-associated virus vectors. Proc Natl Acad Sci USA. 1995; 92(12):5719–23. [PubMed: 7777575]

21. Zhang T, Hu J, Ding W, Wang X. Doxorubicin augments rAAV-2 transduction in rat neuronal cells. Neurochem Int. 2009; 55(7):521–8. [PubMed: 19450628]
22. Hansen J, Qing K, Srivastava A. Adeno-associated virus type 2-mediated gene transfer: altered endocytic processing enhances transduction efficiency in murine fibroblasts. J Virol. 2001; 75(9): 4080–90. [PubMed: 11287557]
23. Ju XD, Lou SQ, Wang WG, Peng JQ, Tian H. Effect of hydroxyurea and etoposide on transduction of human bone marrow mesenchymal stem and progenitor cell by adeno-associated virus vectors. Acta Pharmacol Sin. 2004; 25(2):196–202. [PubMed: 14769209]
24. Cheng B, Ling C, Dai Y, Lu Y, Glushakova LG, Gee SW, et al. Development of optimized AAV3 serotype vectors: mechanism of high-efficiency transduction of human liver cancer cells. Gene Ther. 2012; 19(4):375–84. [PubMed: 21776025]
25. Denby L, Nicklin SA, Baker AH. Adeno-associated virus (AAV)-7 and -8 poorly transduce vascular endothelial cells and are sensitive to proteasomal degradation. Gene Ther. 2005; 12(20): 1534–8. [PubMed: 15944729]
26. Douar AM, Poulard K, Stockholm D, Danos O. Intracellular trafficking of adeno-associated virus vectors: routing to the late endosomal compartment and proteasome degradation. J Virol. 2001; 75(4):1824–33. [PubMed: 11160681]
27. Li W, Zhang L, Wu Z, Pickles RJ, Samulski RJ. AAV-6 mediated efficient transduction of mouse lower airways. Virology. 2011; 417(2):327–33. [PubMed: 21752418]
28. Yan Z, Zak R, Luxton GW, Ritchie TC, Bantel-Schaal U, Engelhardt JF. Ubiquitination of both adeno-associated virus type 2 and 5 capsid proteins affects the transduction efficiency of recombinant vectors. J Virol. 2002; 76(5):2043–53. [PubMed: 11836382]
29. Finn J, Hui D, Downey H, Dunn D, Pien G, Mingozzi F, et al. Proteasome Inhibitors Decrease AAV2 Capsid derived Peptide Epitope Presentation on MHC Class I Following Transduction. Mol Ther. 2009
30. Mitchell AM, Samulski RJ. Mechanistic insights into the enhancement of adeno-associated virus transduction by proteasome inhibitors. J Virol. 2013
31. Del Monte F, Williams E, Lebeche D, Schmidt U, Rosenzweig A, Gwathmey JK, et al. Improvement in survival and cardiac metabolism after gene transfer of sarcoplasmic reticulum Ca(2+)-ATPase in a rat model of heart failure. Circulation. 2001; 104(12):1424–9. [PubMed: 11560860]
32. Adams, J.; Elliott, P.; Bouchard, P. Preclinical Development of Bortezomib (VELCADE®).. In: Adams, J., editor. Proteasome Inhibitors in Cancer Therapy. Humana Press; 2004. p. 233-269.
33. Mariani JA, Smolic A, Preovolos A, Byrne MJ, Power JM, Kaye DM. Augmentation of left ventricular mechanics by recirculation-mediated AAV2/1-SERCA2a gene delivery in experimental heart failure. Eur J Heart Fail. 2011; 13(3):247–53. [PubMed: 21289077]
34. Duan D, Yue Y, Yan Z, Yang J, Engelhardt JF. Endosomal processing limits gene transfer to polarized airway epithelia by adeno-associated virus. J Clin Invest. 2000; 105(11):1573–87. [PubMed: 10841516]
35. Johnson JS, Samulski RJ. Enhancement of adeno-associated virus infection by mobilizing capsids into and out of the nucleolus. J Virol. 2009; 83(6):2632–44. [PubMed: 19109385]
36. Dalkara D, Byrne LC, Lee T, Hoffmann NV, Schaffer DV, Flannery JG. Enhanced gene delivery to the neonatal retina through systemic administration of tyrosine-mutated AAV9. Gene Ther. 2012; 19(2):176–81. [PubMed: 22011645]
37. Qiao C, Yuan Z, Li J, Tang R, Xiao X. Single tyrosine mutation in AAV8 and AAV9 capsids is insufficient to enhance gene delivery to skeletal muscle and heart. Hum Gene Ther Methods. 2012; 23(1):29–37. [PubMed: 22428978]
38. Del Monte F, Butler K, Boecker W, Gwathmey JK, Hajjar RJ. Novel technique of aortic banding followed by gene transfer during hypertrophy and heart failure. Physiol Genomics. 2002; 9(1):49–56. [PubMed: 11948290]
39. Pacher P, Nagayama T, Mukhopadhyay P, Batkai S, Kass DA. Measurement of cardiac function using pressure-volume conductance catheter technique in mice and rats. Nat Protoc. 2008; 3(9): 1422–34. [PubMed: 18772869]

40. Porterfield JE, Kottam AT, Raghavan K, Escobedo D, Jenkins JT, Larson ER, et al. Dynamic correction for parallel conductance, GP, and gain factor, alpha, in invasive murine left ventricular volume measurements. J Appl Physiol. 2009; 107(6):1693–703. [PubMed: 19696357]

41. Baan J, van der Velde ET, de Bruin HG, Smeenk GJ, Koops J, van Dijk AD, et al. Continuous measurement of left ventricular volume in animals and humans by conductance catheter. Circulation. 1984; 70(5):812–23. [PubMed: 6386218]

42. Grimm D, Kern A, Rittner K, Kleinschmidt JA. Novel tools for production and purification of recombinant adenoassociated virus vectors. Hum Gene Ther. 1998; 9(18):2745–60. [PubMed: 9874273]

43. Grieger JC, Choi VW, Samulski RJ. Production and characterization of adeno-associated viral vectors. Nature protocols. 2006; 1(3):1412–28. [PubMed: 17406430]

44. Kohlbrenner E, Henckaerts E, Rapti K, Gordon RE, Linden RM, Hajjar RJ, et al. Quantification of AAV Particle Titers by Infrared Fluorescence Scanning of Coomassie-Stained Sodium Dodecyl Sulfate-Polyacrylamide Gels. Human gene therapy. Part B. Methods. 2012; 23(3):198–203. [PubMed: 22816378]

45. Communal C, Singh K, Pimentel DR, Colucci WS. Norepinephrine stimulates apoptosis in adult rat ventricular myocytes by activation of the beta-adrenergic pathway. Circulation. 1998; 98(13): 1329–34. [PubMed: 9751683]

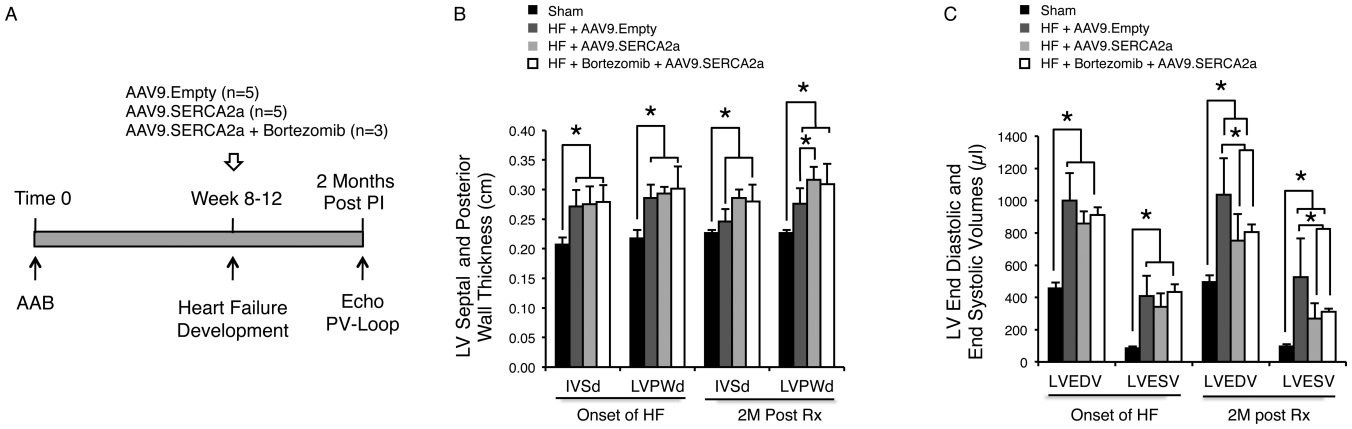

Figure 1. Echocardiography Reveals No Differences in Cardiac Function among Animals with Heart Failure that Were Treated with AAV9.SERCA2a Alone or with AAV9.SERCA2a and Bortezomib

A: Schematic illustration of the study design. **B:** There were no significant differences in septal and posterior wall thickness among the AAV9.Empty and AAV9.SERCA2a with and without bortezomib treated groups. **C:** There were significant decreases in LV end diastolic volume and LV end systolic volume in the AAV9.SERCA2a with and without bortezomib treatment, * = P<0.05.

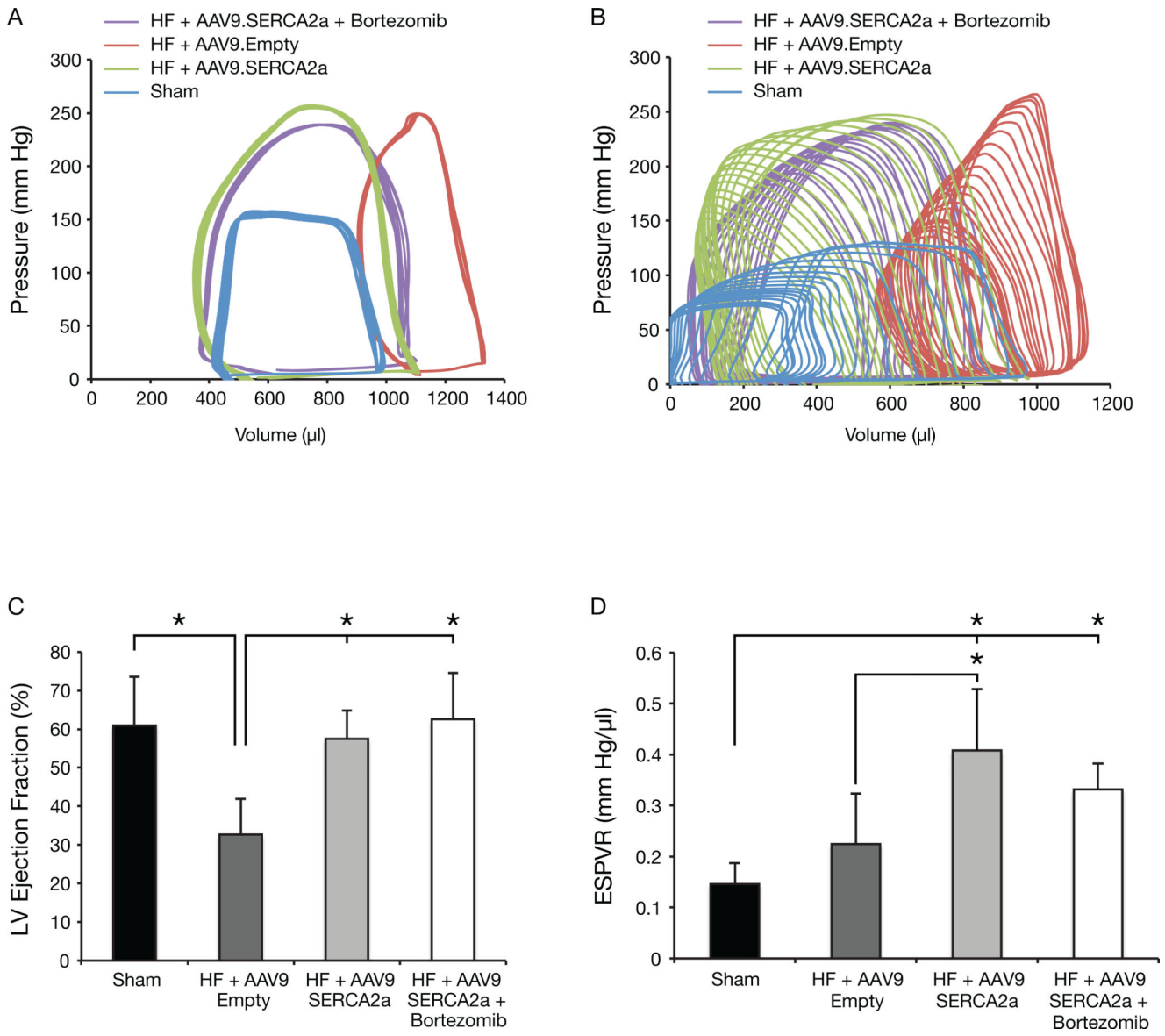

Figure 2. Pressure-Volume Analysis Reveals No Differences in Cardiac Function among Animals with Heart Failure that Were Treated with AAV9.SERCA2a Alone or with AAV9.SERCA2a and Bortezomib

A and B: P-V loop tracings at baseline and during inferior vena cava occlusion. **C:** LV ejection fraction significantly decreased in systolic HF, #P<0.05 vs. sham. **C and D:** Gene transfer of AAV9.SERCA2a with and without bortezomib significantly increased LV ejection fraction and LV contractility, * = P<0.05. The measurements were done at two months post vector injection.

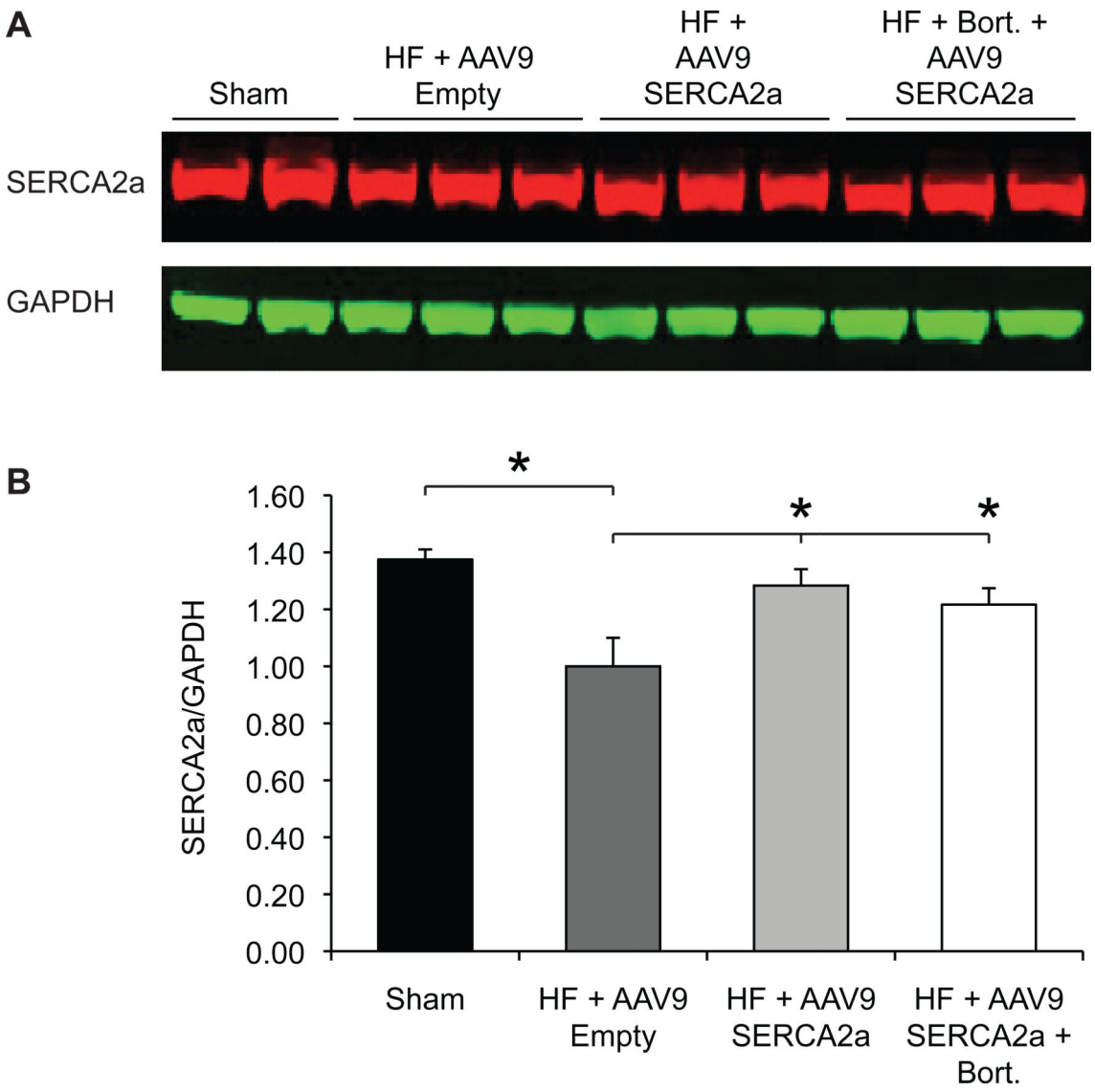

Figure 3. SERCA2a Protein Levels Are Not Different among Animals with Heart Failure that Were Treated with AAV9.SERCA2a Alone or with AAV9.SERCA2a and Bortezomib

A: Western blot analysis of SERCA2a expression. **B:** Quantification of the results in **A.** * = $p<0.05$. The measurements were done at two months post vector injection.

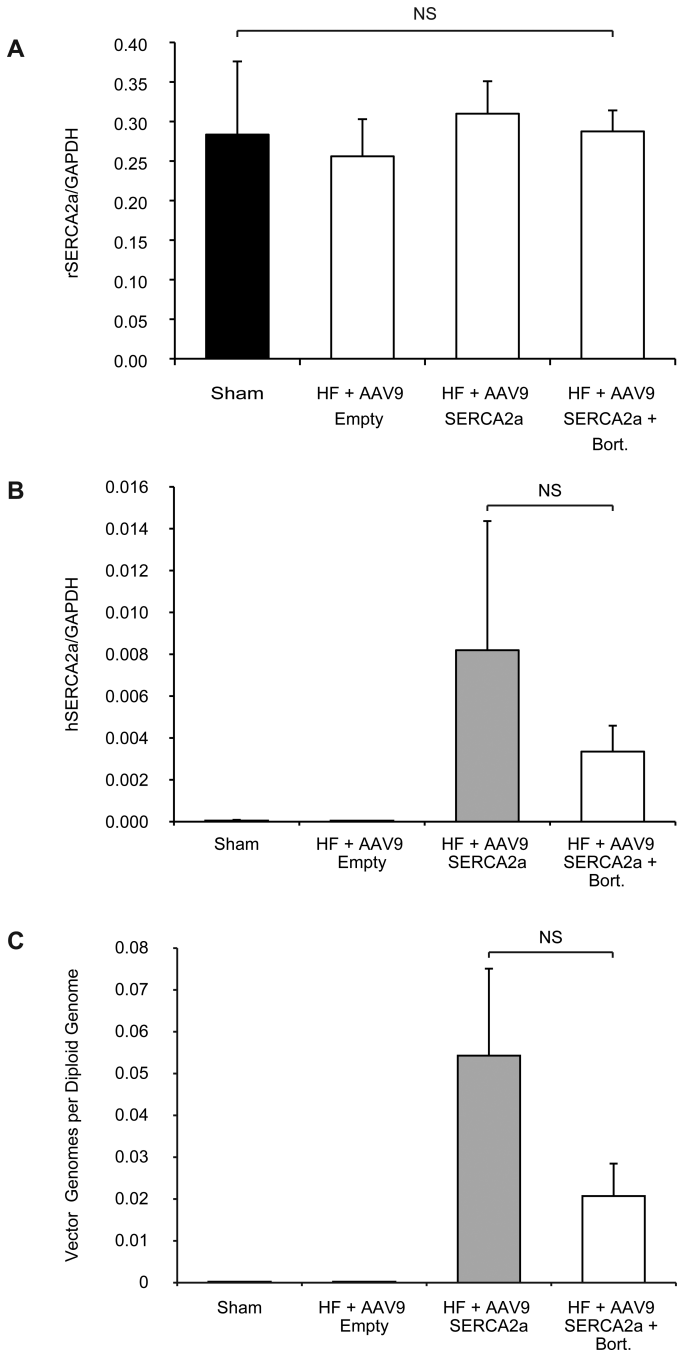

Figure 4. Bortezomib Treatment Does Not Affect Endogenous SERCA2a Expression and Fails to Increase Transduction by AAV9.SERCA2a

A: Rat SERCA2a and GAPDH expression were measured by RT-PCR with specific primers against *rat* SERCA2a and GAPDH. **B:** Human SERCA2a expression was measured with specific primers against *human* SERCA2a and normalized to rat GAPDH expression. **C:** AAV9 vector genomes were normalized to diploid genomes. The measurements were done at two months post vector injection.

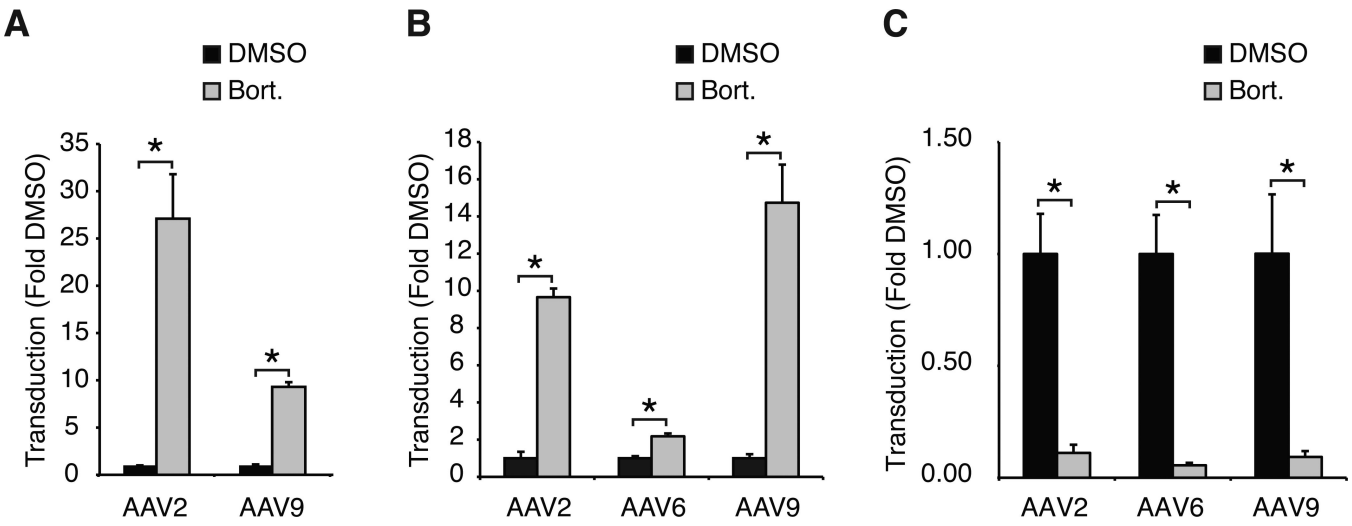

Figure 5. Bortezomib Enhances AAV9 Transduction in HeLa Cells and Neonatal Rat Cardiomyocytes but Decreases Transduction in Adult Rat Cardiomyocytes

A: HeLa cells were pre-treated for 30 minutes with DMSO or bortezomib (1.25 μM) and infected with AAV2-Luciferase or AAV9-Luciferase (1e4 vg/cell). After 24h cells were lysed and firefly luciferase activity was measured. **B:** Neonatal Rat Cardiomyocytes were infected with AAV2-Luciferase, AAV6-Luciferase or AAV9-Luciferase (1e4 vg/cell) in the presence of DMSO or bortezomib (1 μM). Luciferase activity was measured 24h post-infection, **C:** Adult Rat Cardiomyocytes were infected with AAV2-Luciferase, AAV6-Luciferase or AAV9-Luciferase (1e4 vg/cell) in the presence of DMSO or bortezomib (1 μM). Luciferase activity was measured 48h post-infection. * = $p<0.05$.

Table 1

Echocardiography Data of HF Animals Treated with AAV9.Empty vs. AAV9.SERCA2a with or without Bortezomib.

	Onset of Heart Failure				Two Months Post-Injection			
	Sham n=3	**HF + AAV9.Empty n=5**	**HF + AAV9.SERCA2a n=5**	**HF + Bortezomib + AAV9.SERCA2a n=3**	**Sham n=3**	**HF + AAV9.Empty n=5**	**HF + AAV9.SERCA2a n=5**	**HF + Bortezomib + AAV9.SERCA2a n=3**
HW/BW (mg/g)					2.59 ± 0.13[1]	4.47 ± 0.33	4.92 ± 0.45	4.93 ± 0.50
BW (g)	439 ± 45.77	562.71 ± 87.44	478.78 ± 50.65	498.33 ± 44	683 ± 29.43	601.4 ± 67.47	604.67 ± 72.17	538 ± 39.34
IVSd (cm)	0.21 ± 0.01[1]	0.27 ± 0.03	0.28 ± 0.03	0.28 ± 0.03	0.23 ± 0.01[1]	0.26 ± 0.02	0.29 ± 0.01	0.28 ± 0.03
LVPWd (cm)	0.22 ± 0.01[1]	0.29 ± 0.02	0.29 ± 0.01	0.30 ± 0.04	0.23 ± 0.01[1]	0.28 ± 0.03	0.32 ± 0.02	0.31 ± 0.03
LVIDd (cm)	0.68 ± 0.04[1]	0.87 ± 0.06	0.85 ± 0.05	0.84 ± 0.05	0.72 ± 0.03[1]	0.91 ± 0.10	0.82 ± 0.05	0.85 ± 0.06
LVIDs (cm)	0.27 ± 0.02[1]	0.5 ± 0.06	0.5 ± 0.07	0.47 ± 0.04	0.29 ± 0.03[1]	0.55 ± 0.10[2]	0.43 ± 0.06	0.43 ± 0.03
LVFS (%)	59.41 ± 2.35[1]	42.32 ± 4.77	41.42 ± 6.18	43.70 ± 2.40	59.47 ± 3.01[1]	39.83 ± 6.74[2]	47.60 ± 4.33	49.70 ± 1.47
LVEDV (μl)	455.55 ± 38.37[1]	1002.37 ± 168.51	859.10 ± 74.58	910.48 ± 47.85	495.30 ± 43.31[1]	1038.25 ± 224.41[2]	752.33 ± 164.46	806.32 ± 47.43
LVESV (μl)	84.15 ± 12.79[1]	408.92 ±124.34	341.27 ± 83.27	433.53 ± 46.82	96.17 ± 14.40[1]	525.86 ± 241.45[2]	269.10 ± 96.25	310.90 ± 20.56
LVEF (%)	81.38 ± 3.52[1]	59.59 ± 9.48	60.39 ± 8.09	52.47 ± 3.03	80.70 ± 1.55[1]	51.11 ± 11.02[2]	64.97 ± 4.73	61.45 ± 0.54

There was no significant difference between HF + AAV9.SERCA2a vs HF + AAV9.SERCA2a + bortezomib.

[1] p±0.05 Sham vs. all HF groups (AAV9.Empty, AAV9.SERCA2a ± bortezomib)

[2] p±0.05 HF+ AAV9.Empty vs HF + AAV9.SERCA2a ± bortezomib.

Gene Ther. Author manuscript; available in PMC 2014 October 01.

Table 2

Hemodynamic Data of HF Animals Treated with AAV9.Empty vs. AAV9.SERCA2a with or without Bortezomib.

Hemodynamic data	Maximum pressure (mmHg)	End diastolic pressure (mmHg)	End systolic pressure (mmHg)	EF (%)	ESPVR mmHg/µl	V0 (µl)	EDPVR mmHg/µl
Sham (n=3)	133 ± 26.53[1]	7.4 ± 2.09[1]	119.2 ± 36.69[1]	60.93 ± 12.52	0.15 ± 0.04	−449.80 ± 149.7[1]	0.018 ± 0.01[1]
HF + AAV9.Empty (n=5)	245.67 ± 15.26	20.73 ± 5.19	165.2 ± 11.46	32.67 ± 9.19[2,3]	0.22 ± 0.10	265.41 ± 157.50[2]	0.04 ± 0.02
HF + AAV9.SERCA2a (n=5)	251 ± 15.03	18.27 ± 7.03	177.93 ± 13.45	57.47 ± 7.341	0.41 ± 0.12[4]	−152.34 ± −68.68	0.03 ± 0.01
HF + Bortezomib + AAV9.SERCA2a (n=3)	261.38 ± 19.86	20.66 ± 1.15	178.11 ± 20.1	62.55 ± 121	0.33 ± 0.05[5]	−216.89 ± 85.99	0.037 ± 0.006

[1] p±0.05 Sham vs. HF groups (AAV9.Empty, AAV9.SERCA2a ± bortezomib)

[2] p±0.05 HF + AAV9.Empty vs HF + AAV9.SERCA2a ± bortezomib.

[3] p<0.05 HF + AAV9.Empty vs Sham.

[4] P<0.05 HF + AAV9.SERCA2a vs HF + AAV9.Empty

[5] P= 0.07 HF + AAV9.Empty vs HF + AAV9.SERCA2a + bortezomib.